ACS APPLIED MATERIALS & INTERFACES

Article

Label-Free and Ultrasensitive Biomolecule Detection Based on Aggregation Induced Emission Fluorogen via Target-Triggered Hemin/G-quadruplex-Catalyzed Oxidation Reaction

Haiyin Li, Jiafu Chang, Panpan Gai, and Feng Li

ACS Appl. Mater. Interfaces, **Just Accepted Manuscript** • DOI: 10.1021/acsami.7b18676 • Publication Date (Web): 16 Jan 2018

ACS Publications

ACS Applied Materials & Interfaces is published by the American Chemical Society.
1155 Sixteenth Street N.W., Washington, DC 20036

Label-Free and Ultrasensitive Biomolecule Detection Based on Aggregation Induced Emission Fluorogen via Target-Triggered Hemin/G-quadruplex-Catalyzed Oxidation Reaction

Haiyin Li,[a] *Jiafu Chang,*[a] *Panpan Gai,*[a] *and Feng Li**[ab]

[a] College of Chemistry and Pharmaceutical Sciences, Qingdao Agricultural University, Qingdao, 266109, China

[b] Key Laboratory of Applied Mycology of Shandong Province, Qingdao Agricultural University, Qingdao, 266109, China

* Corresponding author. Tel/Fax: 86-532-86080855; E-mail: lifeng@qust.edu.cn

KEYWORDS: label-free; ultrasensitive; aggregation induced emission; hemin/G-quadruplex; catalyzed oxidation reaction

ABSTRACT

Fluorescence biosensing strategy has drawn substantial attention due to their advantages of simplicity, convenience, sensitivity and selectivity, but unsatisfactory structure stability, low fluorescence quantum yield, high cost of labeling, and strict reaction conditions associated with current fluorescence methods severely prohibit their potential application. To address these challenges, we herein propose an ultrasensitive label-free fluorescence biosensor by integrating hemin/G-quadruplex-catalyzed oxidation reaction with aggregation induced emission (AIE) fluorogen-based system. L-cysteine/TPE-M, which is carefully and elaborately designed and developed, obviously contributes to strong fluorescence emission. In the presence of G-rich DNA along with K^+ and hemin, efficient destruction of L-cysteine occurs due to hemin/G-quadruplex-catalyzed oxidation reactions. As a result, highly sensitive fluorescence detection of G-rich DNA is readily realized, with a detection limit down to 33 pM. As a validation for the further development of the proposed strategy, we also successfully construct ultrasensitive platforms for microRNA, by incorporating the L-cysteine/TPE-M system with target-triggered cyclic amplification reaction. Thus, this proposed strategy is anticipated to find use in basic biochemical research and clinical diagnosis.

INTRODUCTION

It is well established that some important molecules including nucleic acids and proteins, with relatively low concentration in biological samples, correlate with various human diseases (cancers, diabetes, autoimmune diseases, and so on).[1-3] For example, microRNA (miRNA), which is low abundance in total RNA samples and associated with human cancers, neurological disease and viral infections, can act as valuable biomarkers for the biomedical research and evaluation.[4,5] However, it should be pointed out that the design and development of efficient biosensors for low abundant analyte detection in complex samples is still a challenge.

Recently, substantial efforts have been devoted to pursuing novel amplification strategies for developing ultrasensitive bioassays in tracing disease-related biomolecules.[6-12] It has been gradually recognized that the sensitivity mainly depends on the physicochemical properties of signal elements.[13-16] In this context, fluorescence materials that can be implemented as signal molecules have drawn much more attention for their widespread application prospect in chemo-/bioanalysis. However, most signal elements previously reported were mainly comprised of conventional dyes,[17-19] such as fluorescein, rhodamine, cascade blue, and so on, of which the intrinsic aggregation caused quenching (ACQ) effect[20,21] and instability in complicated environments (pH, temperature, interferences, and so on) greatly impeded their practical application in detection of ultratrace amount of analytes in biological samples. In addition, most of the reported bioassays involved the labeling procedure,[22-24] which is expensive, complicated and time consuming, and may influence the hybridizing/binding efficiency of the oligonucleotides because of the bulky groups of the labeling elements,

subsequently reducing the sensing selectivity and sensitivity. With this in mind, it is highly desirable and of great research value to design and prepare fluorescence materials with high quantum yield and exceptional stability for constructing ultrasensitive label-free platforms for advanced utilization in bioanalysis.

Aggregation induced emission (AIE) fluorophores, a paramount member of fluorescent material family, have attracted considerable attention because of their unique photophysical properties, and have found promising application in chemo-/biosensors.[25-29] For instance, Tang et al reported a 2D layered metal-organic framework (MOF) with AIE property to analyze various volatile organic compounds.[28] Liu's group developed a simple but unique fluorescent probe with a dual signal turn-on feature for accurate caspase-3 detection based on AIE fluorogen.[29] In this view, AIE fluorogens enjoy high brightness and excellent stability, and have been proven to be ideal signal molecules for addressing the challenges outlined above and developing ultrasensitive biosensors. Additionally, among different transducer techniques, nucleic acid sensors, implementing oligonucleotides as recognition elements for binding/hybridizing target analytes with high affinity and selectivity, possess the appealing features in terms of easy preparation, ease of functionalization, and unique physicochemical stability, and have shown great potential in the analysis of diverse biomolecules in real samples.[30-33] Inspired by the aforementioned developments, by coupling the merits of AIE fluorogens and nucleic acid techniques, AIE fluorogen-based nucleic acid bioassays with excellent selectivity, high sensitivity, and strong anti-interference ability could be developed. However, up to now, only few approaches using AIE fluorogens as signal molecules were reported for constructing nucleic acid-based sensing platform.[34-38] Moreover, tedious labeling

procedure was still needed in the sensing process.[34] On the other hand, the label-free biosensing strategies ever reported were mainly achieved by using cationic AIE fluorogens as signal molecules, which were easily interfered by the anionic compounds in biological samples, subsequently resulting in poor reproducibility and false positive diagnosis.[35-38] In view of this, it is still very important for researchers to develop ingenious strategies for developing label-free AIE fluorogen-based nucleic acid biosensors with robust stability, good reproducibility, high sensitivity, and excellent selectivity.

Herein, by taking full advantage of both AIE fluorogen and nucleic acid technique, we proposed a novel L-cysteine/AIE fluorogen system as an intrinsic sensing platform, which enjoys the appealing features including remarkable brightness, excellent selectivity, and label-free characteristic, and allows ultrasensitive detection of various analytes based on hemin/G-quadruplex-catalyzed oxidation reaction. In the present study, AIE fluorogen (denoted as TPE-M) was successfully designed and synthesized, and showed negligible fluorescence emission because of the exciton annihilation process associated with the molecular structure. L-cysteine (Figure S1A) was applied as a catalyst to induce the significant fluorescence enhancement of TPE-M due to the damage of the maleimide ring. Hemin/G-quadruplex was found to catalyze the oxidation of L-cysteine into cystine (Figure S1B),[39-41] which could not turn on the fluorescence of TPE-M. Basically, the capability of hemin/G-quadruplex-catalyzed oxidation of L-cysteine into cystine can be implemented as a means to control the fluorescence of L-cysteine/TPE-M system. As a result, highly sensitive detection of G-rich DNA was readily realized. Furthermore, this proposed strategy was implemented in the ultrasensitive analysis of miRNA, as proof-of-concept analyte, which

initiate the amplification reaction to generate abundant G-rich DNAs. Moreover, this strategy can be easily and universally applied to any fluorescence probe with response to L-cysteine, and can be used to determine a variety of target analytes, which trigger the generation of G-rich DNA.

EXPERIMENTAL SECTION

Development of L-cysteine/TPE-M System. TPE-M was dissolved in CH_3CN to yield a stock solution of 400 μM, and L-cysteine was dissolved in Tris-HCl (10 mM Tris, 200 mM NaCl, 20 mM KCl, and pH 8.0) to yield a stock solution of 200 μM. Different amount of L-cysteine sample was added into 10 μL TPE-M solution, and the mixture was then incubated for 20 min. Afterwards, the fluorescence emission spectra of the resulted solution that was diluted to 200 μL by Tris-HCl, were collected ranging from 425 to 650 nm with the excitation wavelength of 365 nm.

Fluorescence Detection of G-rich DNA. In a typical assay, different amount of G-rich DNA sample was added into a 50 μL Tris-HCl solution containing 8.0 μM hemin, and incubated for 45 min in order to form hemin/G-quadruplex complexes. The system was then incubated with 20 μL L-cysteine solution for 30 min to complete the catalyzed oxidation reaction. Subsequently, the reaction solution was added into 10 μL TPE-M solution, and the mixture was allowed to react for 20 min. Finally, the resulting solution was brought to a final volume of 200 μL by adding Tris-HCl before fluorescence measurements.

Fluorescence Detection of miRNA. In this study, the miRNA-initiated cyclic amplification reactions were carried out in a 50 μL homogeneous reaction solution (10 mM Tris, 50 mM NaCl, 10 mM $MgCl_2$, 1.0 mM dithiothreitol, and pH 8.0) consisting of 400 nM

template 1, 800 nM template 2, 2000 μM dNTPs, 1.2 U/μL RNase inhibitor, 0.8 U/μL Nt.BbvCI, 1.2 U/μL KF polymerase, and the target miRNA with different concentrations. After reaction at 37 ^{o}C for 120 min, the reaction solution was then heated to 90 ^{o}C and kept at that temperature for 10 min. After cooling down to room temperature, 50 μL Tris-HCl containing 8.0 μM hemin was added into the system and incubated for 45 min to form the hemin/G-quadruplex complex. Subsequently, 20 μL L-cysteine solution was added, and were allowed to react for 30 min. Afterwards, the mixture was added into 10 μL TPE-M solution to react for 20 min. Finally, the resulting solution was diluted to 200 μL with Tris-HCl before fluorescence measurements.

RESULTS AND DISCUSSION

Development of L-cysteine/TPE-M System. In the present work, AIE fluorogen TPE-M, was prepared according to the previously reported method,[42] with the synthetic route depicted in Figure 1A, and the detailed steps for the synthesis exhibited in Supporting Information. To evaluate the response of TPE-M to L-cysteine, we conducted the fluorescence measurements on TPE-M with different L-cysteine concentrations. As manifested in Figure 1B and 1C, the fluorescence intensity significantly augmented with the increase of L-cysteine concentration, which could be ascribed to the fact that more L-cysteine interacted with more TPE-M, subsequently resulting in delayed or blocked exciton annihilation process. For instance, with the concentration of L-cysteine reached 30 μM, a ca. 9.9-fold increase in fluorescence intensity was observed. In addition, the incubation time between L-cysteine and TPE-M was optimized to be 20 min (Figure S2A). Meanwhile, hardly any change in fluorescence intensity of TPE-M or TPE-M-L can be detected after placing for 120 min, which demonstrated that

TPE-M/TPE-M-L enjoy highly optical stability (Figure S2B). These results evidently suggested that TPE-M enjoyed significant response to L-cysteine. Furthermore, several comparison experiments by using six other compounds were applied to investigate the specific response of TPE-M to L-cysteine, and the detailed information was depicted in Figure S2C. It should be noted that the compounds without –SH, cannot induce the fluorescence enhancement of TPE-M. Oppositely, compounds with –SH, will significantly turn on the fluorescence of TPE-M. This experimental result successfully unveils the critical role of –SH of L-cysteine for turning on the fluorescence of TPE-M. Moreover, the response of TPE-M to L-cysteine was further proven by characterizing the structures of both TPE-M and the TPE-M-L arising from the reaction between TPE-M and L-cysteine through FT-IR and ^{1}H NMR techniques, as demonstrated in Figure S3, and Figure S4. Significant differences were observed, which authenticated that TPE-M possesses prominent response to L-cysteine.

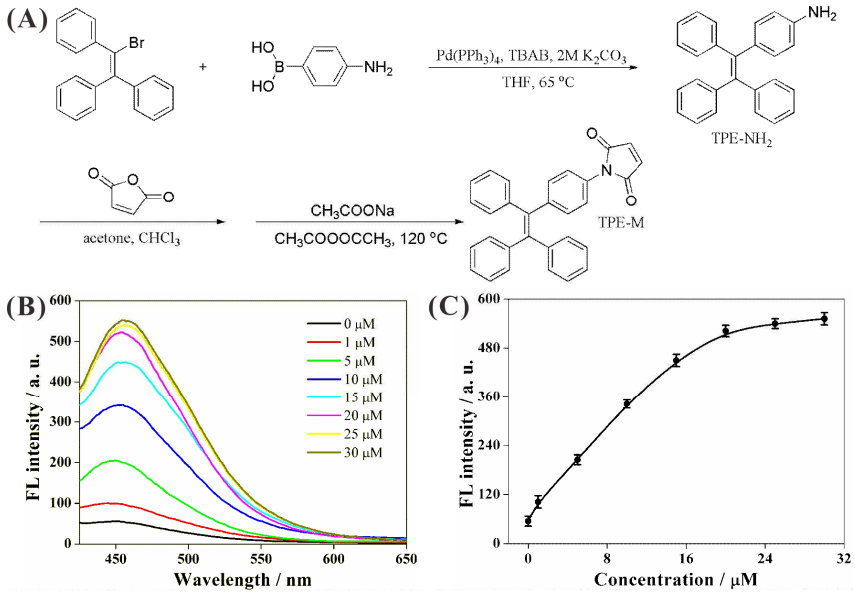

Figure 1. (A) Synthetic route to TPE-M. (B) Fluorescence spectra of TPE-M (20 μM) with different concentrations of L-cysteine. (C) Fluorescence intensity of

L-cysteine/TPE-M system versus the concentration of L-cysteine.

Development of L-cysteine/TPE-M-Based Biosensor for G-rich DNA Detection. Based on the proposed L-cysteine/TPE-M system, the general platform for sensitive G-rich DNA detection through hemin/G-quadruplex-controlled the fluorescence of TPE-M was developed and the working principle was illustrated in Figure 2A. Evidently, in the absence of hemin/G-quadruplex, L-cysteine could not be oxidized to cystine, and still maintained the capability to turn on the fluorescence of TPE-M. As a result, a significant signal was acquired. However, in the presence of G-rich DNA, L-cysteine was effectively converted into cystine *via* the catalyzed oxidation reaction of hemin/G-quadruplex.[39-41] Because the generated cystine did not enjoy the ability to turn on TPE-M's fluorescence, much lower fluorescence intensity was detected compared with that of L-cysteine/TPE-M in the absence of G-rich DNA. Since the fluorescence signal was dependent on the amount of L-cysteine, which was subsequently relied on the concentration of G-rich DNA, fluorescence signal of the proposed bioassay was related to the concentration of target G-rich DNA, and sensitive fluorescence detection of G-rich DNA was readily realized.

To investigate the feasibility of the proposed strategy, fluorescence spectra of the sensing system under different conditions were recorded and displayed in Figure 2B, using G1 (G-rich DNA) as the proof-of-concept analyte. Obviously, a relatively weak fluorescence signal (88.2 a. u.) was observed when G1 was pre-incubated with L-cysteine in the presence of K^+ and hemin (curve e). It came as no surprise due to the sensing principle that is based on the ability of hemin/G-quadruplex to effectively catalyze oxidation of L-cysteine into cystine, as well as cystine's inability to turn on the fluorescence of TPE-M. The ability of

hemin/G-quadruplex-catalyzed oxidation of L-cysteine to cystine was affirmed by horseradish peroxidase (HRP) in the presence of H_2O_2 (Figure S5). Whereas, strong fluorescence emission was observed in the absence of either G1 (curve c) or hemin (curve d), due to the fact that no hemin/G-quadruplex complex was formed, and L-cysteine was intact, and still maintained its ability to react with TPE-M. Thus, numerous fluorescent molecules (TPE-M-L) were generated in the system and resulted in strong fluorescence. These experimental results clearly demonstrated that the fluorescence detection of G-rich DNA could be readily realized using the proposed system.

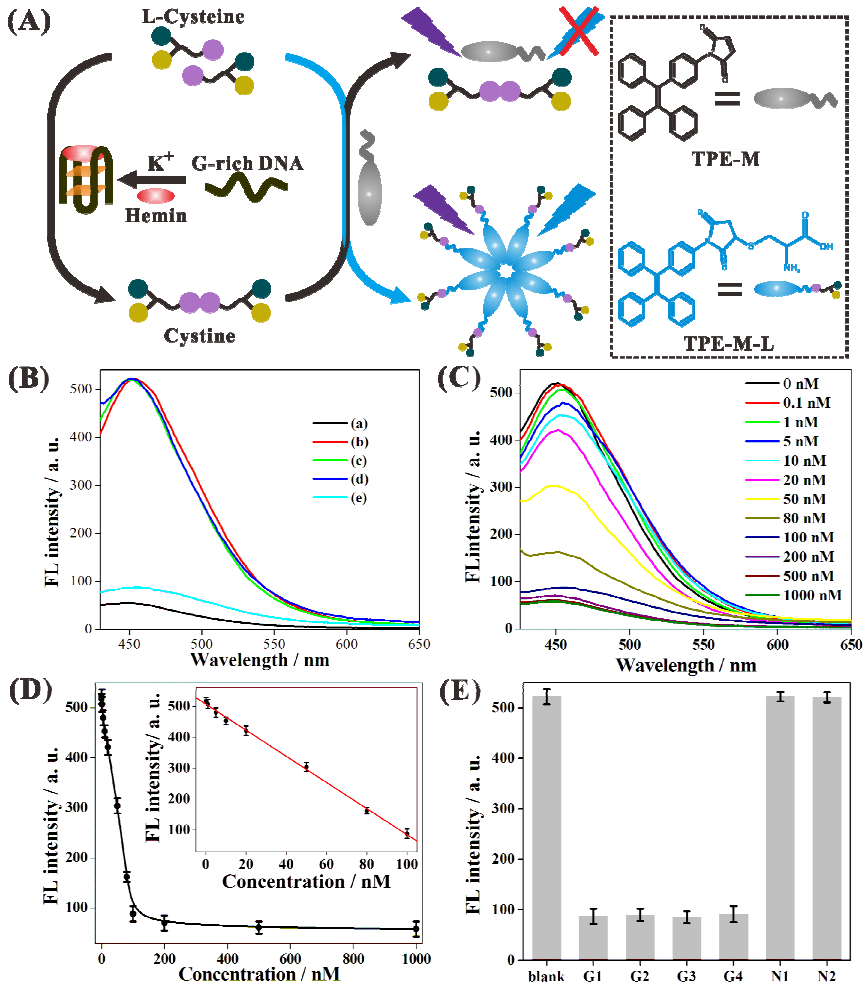

Figure 2. (A) Schematic illustration of the principle of L-cysteine/TPE-M-based biosensor for G-rich DNA detection. (B) Fluorescence spectra of L-cysteine/TPE-M-based biosensor under

different conditions: (a) TPE-M, (b) TPE-M + L-cysteine, (c) TPE-M + L-cysteine + hemin, (d) TPE-M + L-cysteine + G1, (e) TPE-M + L-cysteine + hemin + G1. (C) Fluorescence spectra of the proposed biosensor upon the addition of G1 with different concentrations. (D) The fluorescence intensity of the proposed bioassay versus the G1 concentration. Inset: the linear relationship between fluorescence intensity and the G1 concentration. (E) Comparison of the fluorescence intensity in the presence of G1, G2, G3, G4, N1, and N2, respectively, in which "blank" indicates the condition in the absence of any analyte. The concentrations of TPE-M, L-cysteine, hemin, and G-rich DNA (G1, G2, G3, and G4) were 20 μM, 20 μM, 2.0 μM, and 100 nM, respectively; the concentrations of N1 and N2 were 1000 nM.

Under the optimum sensing conditions (Detail optimizations are shown in Figure S6A and 6B), we challenged this fluorescence bioassay by probing G1 with different concentrations to test its analytical performance. As expected, the fluorescence intensity decreased gradually with the increased G1 concentration, which was attributed to the fact that more G1 impelled the formation of more hemin/G-quadruplex complexes and reduced the amount of L-cysteine, subsequently resulting in the fluorescence decrease (Figure 2C). Evidently, G1 with the concentrations ranging from 0.1 to 1000 nM could be directly detected by the proposed system (Figure 2D). Furthermore, the fluorescence intensity was linearly dependent on G1 concentration ranging from 0.1 to 100 nM (Figure 2D, inset). The resulting linear regression equation was determined to be $F = -4.23C_{G1} + 507.19$ (F in the unit of a. u., and C_{G1} in the unit of nM), with the correlation coefficient of R^2=0.9988. The measured detection limit was determined to be 33 pM, which is superior or comparable to those of the methods for G-rich DNA detection reported in literature (Table S2). These results arguably confirmed the AIE fluorogen-assisted effective enhancement of detection efficiency for target analyte.

According to the mechanism of the proposed bioassay, the developed approach was expected to be effective in analyzing other G-rich DNAs, which contributed to the formation of hemin/G-quadruplex in the presence of K^+ and hemin. To gain more insight, we tested the fluorescence signal of the proposed system upon the addition of different DNA strands, namely G2, G3, G4, N1, and N2, respectively. G2, G3, and G4 were designed to comprise of G-rich sequences, whereas, N1 and N2 did not contain G-rich elements. As depicted in Figure 2E, significant decrease in fluorescence intensity was only observed in the presence of G-rich DNAs (G1, G2, G3 and G4). In contrast, hardly any fluorescence change could be detected in the presence of N1 or N2, even though the concentration was ten times as many as G-rich DNA. These results justified the crucial role of G-rich DNA in controlling the fluorescence of L-cysteine/TPE-M system, and suggested that this fluorescence biosensor was applicable for the determination of any G-rich DNA that could fold into G-quadruplex structure.

Based on the ability of hemin/G-quadruplex to control the fluorescence of L-cysteine/TPE-M system, effective design and development of novel sensing platform for detecting various biomolecules can be realized. Meanwhile, it is well known that enzyme-assisted signal amplification strategy is another key component involved in the achievement of ultrasensitive biosensor.[43-46] Hence, a target-initiated cyclic amplification strategy, is carefully and ingeniously integrated with the proposed system for the construction of ultrasensitive fluorescence platforms. This is exemplified here with the probing of miRNA using our developed system.

Development of L-cysteine/TPE-M-Based Biosensor for Ultrasensitive miRNA Detection. Figure 3A gives the layout for the ultrasensitive analysis of miRNA based on the

target-initiated isothermal exponential amplification reaction (EXPAR) and hemin/G-quadruplex-controlled turning on the fluorescence of L-cysteine/TPE-M system. In this study, template 1 and 2 were carefully and elaborately designed to avoid any spontaneous interaction between each other in the absence of target miRNA. Template 1 contains three regions (I, II, and III) separated by two nicking endonuclease recognition sequences, of which region I and II have the identical sequences complementary to target miRNA. Template 2 also comprises of three regions (I′, II′, and III′) separated by two nicking endonuclease recognition sequences, of which region I′ and II′ have the identical sequences with that of region III in template 1, and region III′ composes the sequences complementary to G-rich DNA. As depicted in Figure 3B, both the template 1 and 2 exhibited a single and narrow electrophoresis band (lane a and b), respectively, implying that no secondary structure generated in each of the carefully designed DNA strands. Moreover, mixing template 1 and 2 did not generate any new band in the absence of miRNA (lane c), suggesting the low degree of spontaneous reaction between template 1 and 2.

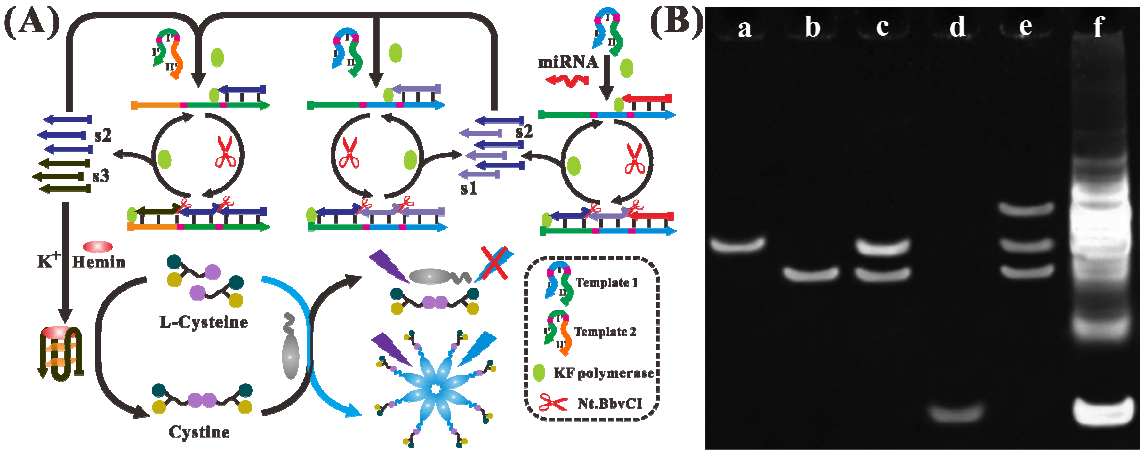

Figure 3. (A) Schematic illustration of the principle of L-cysteine/TPE-M-based biosensor for ultrasensitive miRNA detection through target-switched EXPAR reaction. (B) Nondenaturing

PAGE images of (a) template 1, (b) template 2, (c) template 1 + template 2, (d) G1, (e) let-7a + template 1 + template 2, (f) let-7a + template 1 + template 2 + KF polymerase + dNTPs + Nt. BbVCl.

In the presence of target analyte, the hybridization between miRNA and the complementary region in template 1 resulted in a conformational change of template 1 from single strand structure to miRNA-hybridizing structure. As seen from lane e in Figure 3B, the newly appeared band, at the shorter distance than that of template 1, was associated with the formation of miRNA-template 1 complex, arising from the specific hybridization reaction. In this case, target miRNA acted as primer to trigger the EXPAR reactions from its 3′-end in the presence of KF polymerase, dNTPs, and Nt. BbVCl., releasing DNA triggers s1 and s2. Owing to the ingenious design, the s1 hybridized to unreacted template 1 to initiate more EXPAR reactions to generate more s2, which, in turn, hybridized to template 2 and acted as primers to trigger the EXPAR reactions. The successful target-initiated EXPAR reactions would generate a large number of DNA triggers s3. As expected, lane f in Figure 3B showed multiple new electrophoresis bands at different distances, of which the fastest-moving electrophoresis band was related to the generated s3 that was justified by the electrophoresis band of G1 (lane d). Therefore, plentiful hemin/G-quadruplexes were formed in the presence of K^+ and hemin, and catalyzed oxidation of L-cysteine into cystine, subsequently resulting in the fluorescence decrease. While in the absence of miRNA, template 1 and 2 were incapable of any interaction, inhibiting the subsequent EXPAR reactions. In this context, L-cysteine would not be consumed, and would maintain its ability to turn on the fluorescence of TPE-M, contributing to strong fluorescence signal. Thus, by monitoring the change in fluorescence

intensity, we could determine the target miRNA with ultrahigh sensitivity based on the proposed AIE fluorogen-based system by incorporating the EXPAR reactions.

To verify the feasibility of the proposed strategy, the fluorescence signals of the sensing system under different conditions were obtained and depicted in Figure 4A. Obviously, a strong fluorescence signal was observed when target let-7a was absent (curve c), with the intensity of about 516.9 a. u. This phenomenon arguably supported the conclusion that template 1, template 2, KF polymerase, dNTP, and Nt. BbVCl have little effect on the fluorescence of L-cysteine/TPE-M system. Upon the addition of let-7a with different concentrations, the fluorescence intensity decreased from 516.9 a. u. (curve c) to 293.1 a. u. (curve d) and 163.8 a. u. (curve e), respectively. This is because a large number of hemin/G-quadruplexes were formed upon the miRNA-initiated EXPAR reactions, and the generated hemin/G-quadruplex enjoyed significantly catalyzed oxidation ability toward L-cysteine. These results clearly justified the feasibility of the proposed L-cysteine/TPE-M system for sensitive detection of target let-7a.

Next, under the optimum experimental conditions (Detail optimizations are shown in Figure S7), we challenged this fluorescence bioassay by sensing target let-7a with different concentrations to test its analytical performance. As depicted in Figure 4B, the fluorescence intensity significantly decreased with the increase of let-7a concentration, which was attributed to the sensing principle that more let-7a induced the generation of more hemin/G-quadruplexes, and then decreased the amount of L-cysteine, thus reducing the fluorescence intensity. A calibration curve was fitted between *F* (fluorescence intensity in the presence of let-7a with different concentrations) and the logarithm of the let-7a concentration

over a linear range of 0.1 fM to 10000 fM (Figure 4C). The linear equation was calculated to be F = -67.28 log $C_{let\text{-}7a}$ + 431.14 (F in the units of a. u., $C_{let\text{-}7a}$ in the units of fM), with the correlation coefficient of R^2 = 0.9994. The measured detection limit was determined to be 35 aM, which, as shown in Table S3, to the best of our knowledge, was the lowest detection limit ever obtained for let-7a. Evidently, the proposed bioassay is superior in sensitivity to other sensing strategies. The improved sensitivity of the current biosensor might be attributable to the following factors: 1) AIE fluorogen introduced as signal molecule, 2) signal amplification induced by EXPAR reactions, and 3) the highly catalyzed oxidation ability of hemin/G-quadruplex toward L-cysteine.

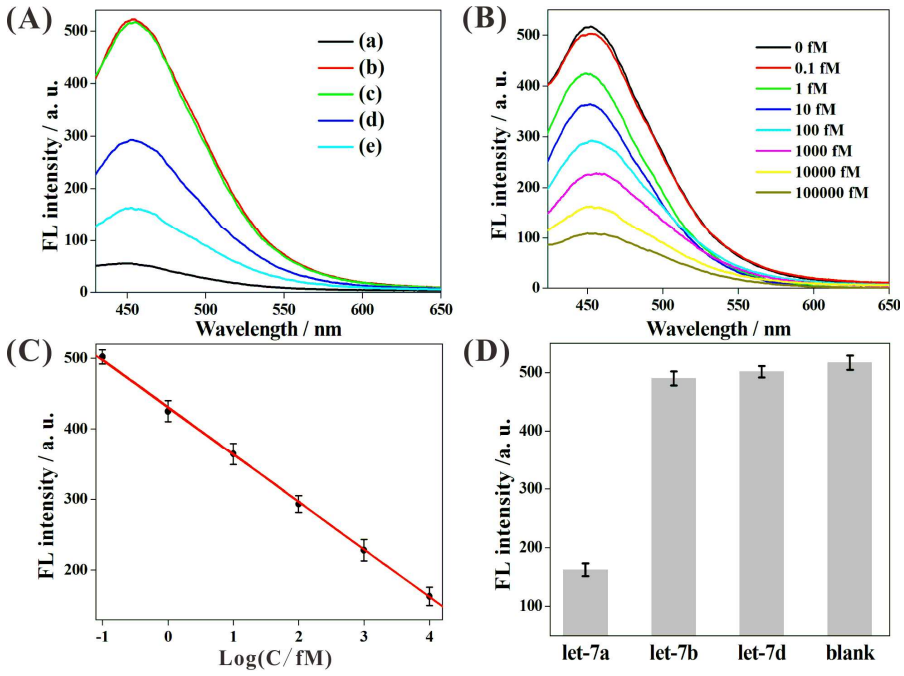

Figure 4. (A) Fluorescence spectra of L-cysteine/TPE-M-based biosensor under different conditions: (a) TPE-M, (b) TPE-M + L-cysteine, (c) TPE-M + L-cysteine + template 1 + template 2 + KF polymerase + Nt. BbVCl. + dNTPs + hemin, (d) TPE-M + L-cysteine + let-7a (100 fM) + template 1 + template 2 + KF polymerase + Nt. BbVCl. + dNTPs + hemin, (e) TPE-M + L-cysteine + let-7a (10000 fM) + template 1 + template 2 + KF polymerase + Nt.

BbVCl. + dNTPs + hemin. (B) Fluorescence spectra of the proposed biosensor upon the addition of let-7a with different concentrations. (C) The linear relationship between the fluorescence intensity and the logarithm of let-7a concentration. (D) Comparison of the fluorescence intensity in the presence of let-7a, let-7b, and let-7d, respectively, in which "blank" indicates the condition in the absence of any analyte. The concentrations of all analytes were 10000 fM.

The selectivity of the proposed bioassay was further investigated by adding let-7a, let-7b and let-7d with the same concentration into the sensing system, respectively. As illustrated in Figure 4D, relatively high fluorescence intensity was detected in the presence of let-7b or let-7d, whereas a significant drop of fluorescence signal was obtained when let-7a was present. The results implied that the proposed strategy demonstrated a high selectivity toward the target let-7a, and was able to distinguish miRNA family members with sequence homology. Meanwhile, the practical application of this method for quantitative miRNA assay in complex biological matrix was studied by determining the recovery of target let-7a spiked in 10% diluted human serum samples. As shown in Table 1, for let-7a at different concentrations of 1.0, 10, and 100 fM, there was good agreement between the added and measured values of let-7a, and the recoveries were found to be in the range of 97–105.1%. These results significantly implied that the proposed label-free fluorescent platform demonstrates potential for application in miRNA detection in human serum samples with acceptable accuracy and good reliability.

Table 1 Detection of let-7a spiked in serum samples (n = 3)

Sample No.	Added (fM)	Mean measured (fM)	Mean recovery [a] (%)
1	1.0	0.97	97
2	10	10.3	103
3	100	105.1	105.1

[a]Recovery (%) = $100 \times (c_{\text{mean measured}} / c_{\text{added}})$

CONCLUSIONS

In summary, a well-designed AIE fluorogen-based stimuli-responsive system (L-cysteine/TPE-M) was successfully developed, and in the presence of hemin/G-quadruplex, it underwent cystine generation associated with fluorescence abatement due to the deactivation of AIE molecules by virtue of HRP-mimicking DNAzyme-catalyzed oxidation of L-cysteine. Thus, L-cysteine/TPE-M system readily acts as an efficient fluorescence bioassay for G-rich DNA detection that can fold into G-quadruplex, with reduced cost, improved probing sensitivity, and enhanced detection selectivity, as compared to previously reported G-rich DNA biosensors. We further demonstrate that L-cysteine/TPE-M system can also be configured into ultrasensitive bioassays for miRNA sensing with the aid of target-initiated cyclic amplification reactions, serving as signal element and offering exceptional stability and excellent selectivity. Overall, the conceptual integration of DNAzyme-catalyzed oxidation reactions with AIE fluorogen-based system represents a versatile and ingenious strategy to construct fluorescence platform with the unique features of label free, low cost, high sensitivity and good selectivity.

Notes

The authors declare no competing financial interest.

ACKNOWLEDGEMENTS

This work was funded by the National Natural Science Foundation of China (Nos. 21605093, 21605092, and 21775082), and the Special Foundation for Distinguished Taishan Scholar of Shandong Province (No. ts201511052).

ASSOCIATED CONTENT

Supporting Information Available: Reagents and apparatus; synthetic information of TPE-M and TPE-M-L; Sequences of the oligonucleotides; assay performance comparison of our strategy with other methods; optimal experimental conditions. These materials are available free of charge via the Internet at http://pubs.acs.org.

REFERENCES

(1) Hopkins, M. M.; Hogarth, S. Biomarker Patents for Diagnostics: Problem or Solution? *Nat. Biotechnol.* **2012**, *30*, 498−500.

(2) Kwok, R. T.; Leung, C. W.; Lam, J. W.; Tang, B. Z. Biosensing By Luminogens with Aggregation-Induced Emission Characteristics. *Chem. Soc. Rev.* **2015**, *44*, 4228−4238.

(3) Arya, S. K.; Bhansali, S. Lung Cancer and Its Early Detection Using Biomarker-Based Biosensors. *Chem. Rev.* **2011**, *111*, 6783−6809.

(4) Wark, A. W.; Lee, H. J.; Corn, R. M. Multiplexed Detection Methods for Profiling MicroRNA Expression in Biological Samples. *Angew. Chem. Int. Ed.* **2008**, *47*, 644−652.

(5) Wu, L.; Qu, X. G. Cancer Biomarker Detection: Recent Achievements and Challenges. *Chem. Soc. Rev.* **2015**, *44*, 2963−2997.

(6) Wang, M.; He, B. Y.; Lu, L. H.; Leung, C. H.; Mergny, J. L.; Ma, D. L. Label-free Luminescent Detection of LMP1 Gene Deletion Using an Intermolecular G-quadruplex-Based Switch-on Probe. Biosens. Bioelectron. 2015, 70, 338–344.

(7) Ma, W.; Fu, P.; Sun, M. Z.; Xu, L. G.; Kuang, H.; Xu, C. L. Dual Quantification of MicroRNAs and Telomerase in Living Cells. J. Am. Chem. Soc. 2017, 139, 11752–11759.

(8) Ying, Z. M.; Wu, Z.; Tu, B.; Tan, W. H.; Jiang, J. H. Genetically Encoded Fluorescent RNA Sensor for Ratiomatric Imaging of MicroRNA in Living Tumor Cells. J. Am. Chem. Soc. 2017, 139, 9779–9782.

(9) Deng, R. J.; Tang, L. H.; Tian, Q. Q.; Wang, Y.; Lin, L.; Li, J. H. Toehold-initiated Rolling Circle Amplification for Visualizing Individual MicroRNAs In Situ in Single Cells. *Angew. Chem. Int. Ed.* **2014**, *53*, 2389−2393.

(10) Liu, Q. Y.; Yang, Y. T.; Li, H.; Zhu, R. R.; Shao, Q.; Yang, S. G.; Xu, J. J. NiO Nanoparticles Modified with 5,10,15,20-Tetrakis(4-Carboxyl Phenyl)-Porphyrin: Promising

Peroxidase Mimetics for H_2O_2 and Glucose Detection. *Biosens. Bioelectron.* **2015**, *64*, 147−153.

(11) Liu, X. Q.; Wang, F.; Aizen, R.; Yehezkeli, O.; Willner, I. Graphene Oxide/Nucleic-Acid-Stabilized Silver Nanoclusters: Functional Hybrid Materials for Optical Aptamer Sensing and Multiplexed Analysis of Pathogenic DNAs. *J. Am. Chem. Soc.* **2013**, *135*, 11832−11839.

(12) Li, H. Y.; Chang, J. F.; Hou, T.; Li, F. HRP-Mimicking DNAzyme-Catalyzed in Situ Generation of Polyaniline To Assist Signal Amplification for Ultrasensitive Surface Plasmon Resonance Biosensing. *Anal. Chem.* **2017**, *89*, 673−680.

(13) Li, J.; Li, D. X.; Yuan, R.; Xiang, Y. Biodegradable MnO_2 Nanosheet-Mediated Signal Amplification in Living Cells Enables Sensitive Detection of Down-Regulated Intracellular MicroRNA. *ACS Appl. Mater. Interfaces.* **2017**, *9*, 5717–5724.

(14) Li, D. X.; Zhou, W. J.; Yuan, R.; Xiang, Y. A DNA-Fueled and Catalytic Molecules Machine Lights Up Trace Under Expressed MicroRNAs in Living Cells. *Anal.Chem.* **2017**, *89*, 9934–9940.

(15) Yu, J. B.; Rong, Y.; Kuo, C. T.; Zhou, X. H.; Chiu, D. T. Recent Advances in the Development of Highly Luminescent Semiconducting Polymer Dots and Nanoparticles for Biological Imaging and Medicine. *Anal. Chem.* **2017**, *89*, 42−56.

(16) Liu, Q. Y.; Yang, Y. T.; Lv, X. T.; Ding Y. N.; Zhang, Y. Z.; Xu, J. J.; Xu. C. X. One-Step Synthesis of Uniform Nanoparticles of Porphyrin Functionalized Ceria with Promising Peroxidase Mimetics for H2O2 and Glucose Colorimetric Detection. *Sensors. Actuat. B-Chem.* **2017**, *240*, 726−734.

(17) Huang, J.; Wang, H.; Yang, X. H.; Quan, K.; Yang, Y. J.; Ying, L.; Xie, N. L.; Ou, M.; Wang, K. M. Fluorescence Resonance Energy Transfer-Based Hybridization Chain Reaction for In Situ Visualization of Tumor-Related miRNA. *Chem. Sci.* **2016**, *7*, 3829−3835.

(18) Hong, M.; Xu, L. D.; Xue, Q. W.; Li, L.; Tang, B. Fluorescence Imaging of Intracellular Telomerase Activity Using Enzyme-Free Signal Amplification. *Anal. Chem.* **2016**, *88*, 12177−12182.

(19) Kang, J.; Loew, M.; Arbuzova, A.; Andreou, I.; Dahne, L. Nucleic Acid Diagnostic FRET Particles Based on Layer-by-Layer Technology. *Adv. Mater.* **2010**, *22*, 3548−3552.

(20) Mei, J.; Leung, N. L. C.; Kwok, R. T. K.; Lam, J. W. Y.; Tang, B. Z. Aggregation-Induced Emission: Together We Shine, United We Soar! *Chem. Rev.* **2015**, *115*, 11718−11940.

(21) Wang, X. R.; Hu, J. M.; Zhang, G. Y.; Liu, S. Y. Highly Selective Fluorogenic Multianalyte Biosensors Constructed via Enzyme-Catalyzed Coupling and Aggregation-Induced Emission. *J. Am. Chem. Soc.* **2014**, *136*, 9890−9893.

(22) Ou, M.; Huang, J.; Yang, X. H.; Quan, K.; Yang, Y. J.; Xie, N. L.; Wang, K. M. MnO_2 Nanosheet Mediated "DD-A" FRET Binary Probes for Sensitive Detection of Intracellular mRNA. *Chem. Sci.* **2017**, *8*, 668−673.

(23) Zhang, X. R.; Li, R. J.; Chen, Y. Y.; Zhang, S. S.; Wang, W. S.; Li, F. C. Applying DNA Rolling Circle Amplification in Fluorescence Imaging of Cell Surface Glycans Labeled by A Metabolic Method. *Chem. Sci.* **2016**, *7*, 6182−6189.

(24) Wang, H.-B.; Wu, S.; Chu, X.; Yu, R.-Q. A Sensitive Fluorescence Strategy for Telomerase Detection in Cancer Cells Based on T7 Exonuclease-Assisted Target Recycling Amplification. *Chem. Commun.* **2012**, *48*, 5916−5918.

(25) Shi, J.; Deng, Q. C.; Wan, C. J.; Zheng, M. M.; Shi, J.; Tang, B. Fluorometric probing lipase levels as acute pancreatitis biomarker based on interfacial controlled aggregation-induced emission (AIE). *Chem. Sci.* **2017**, *8*, 6188–6195.

(26) Li, H. Y.; Chang, J. F.; Hou, T.; Li, F. Aggregation Induced Emission Amphiphile with An Ultra Low Critical Micelle Concentration: Fabrication, Self Assembling, And Cell Imaging. *J. Mater. Chem. B.* **2016**, *4*, 198−201.

(27) Li, H. Y.; Wang, C. F.; Hou, T.; Li, F. Amphiphile-Mediated Ultrasmall Aggregation Induced Emission Dots for Ultrasensitive Fluorescence Biosensing. *Anal. Chem.* **2017**, *89*, 9100−9107.

(28) Zhang, M.; Feng, G. X.; Song, Z. G.; Zhou, Y. P.; Chao, H. Y.; Yuan, D. Q.; Tan, T. T. Y.; Guo, Z. G.; Hu, Z. G.; Tang, B. Z.; Liu, B.; Zhao, D. Two-Dimensional Metal–Organic Framework with Wide Channels and Responsive Turn-On Fluorescence for the Chemical Sensing of Volatile Organic Compounds. *J. Am. Chem. Soc.* **2014**, *136*, 7241−7244.

(29) Yuan, Y. Y.; Zhang, R. Y.; Cheng, X. M.; Xu, S. D.; Liu, B. A FRET Probe with AIEgen as The Energy Quencher: Dual Signal Turn-on for Self-Validated Caspase Detection. *Chem. Sci.* **2016**, *7*, 4245−4250.

(30) Lei, C. Y.; Huang, Y.; Nie, Z.; Hu, J.; Li, L. J.; Lu, G. Y.; Han, Y. T.; Yao, S. Z. A Supercharged Fluorescent Protein as a Versatile Probe for Homogeneous DNA Detection and Methylation Analysis. *Angew. Chem. Int. Ed.* **2014**, *53*, 8358−8362.

(31) Lu, C. H.; Cecconello, A.; Willner, I. Recent Advances in the Synthesis and Functions of Reconfigurable Interlocked DNA Nanostructures. *J. Am. Chem. Soc.* **2016**, *138*, 5172−5185.

(32) Smith, S. J.; Nemr, C. R.; Kelley, S. O. Chemistry-Driven Approaches for Ultrasensitive

Nucleic Acid Detection. *J. Am. Chem. Soc.* **2017**, *139*, 1020−1028.

(33) Yang, C. Y.; Dou, B. T.; Yang, J. M.; Yuan, R.; Xiang, Y. Cross-Triggered and Cascaded Recycling Amplification for Ultrasensitive Electrochemical Sensing of the Mutant Human p53 Gene. *Chem. Commun.* **2016**, *52*, 8707−8710.

(34) Chen, J.; Jiang, H.; Zhou, H. P.; Hu, Z. Z.; Niu, N.; Shahzad, S. A.; Yu, C. Specific Detection of Cancer Cells Through Aggregation-Induced Emission of A Light-up Bioprobe. *Chem. Commun.* **2017**, *53*, 2398−2401.

(35) Xu, X. M.; Hou, R. Z.; Gao, P. C.; Miao, M.; Lou, X. D.; Liu, B. F.; Xia, F. Highly Robust Nanopore-Based Dual-Signal-Output Ion Detection System for Achieving Three Successive Calibration Curves. *Anal. Chem.* **2016**, *88*, 2386−2391.

(36) Zhuang, Y.; Huang, F. J.; Xu, Q.; Zhang, M. S.; Lou, X. D.; Xia, F. Facile, Fast-Responsive, and Photostable Imaging of Telomerase Activity in Living Cells with a Fluorescence Turn-On Manner. *Anal. Chem.* **2016**, *88*, 3289−3294.

(37) Zhuang, Y.; Shang, C. L.; Lou, X. D.; Xia, F. Construction of AIEgens-Based Bioprobe with Two Fluorescent Signals for Enhanced Monitor of Extracellular and Intracellular Telomerase Activity. *Anal. Chem.* **2017**, *89*, 2073−2079.

(38) Zhuang, Y.; Zhang, M. S.; Chen, B.; Duan, R. X.; Min, X. H.; Zhang, Z. Y.; Zheng, F. X.; Liang, H. G.; Zhao, Z. J.; Lou, X. D.; Xia, F. Quencher Group Induced High Specificity Detection of Telomerase in Clear and Bloody Urines by AIEgens. *Anal. Chem.* **2015**, *87*, 9487−9493.

(39) Sharon, E.; Golub, E.; Niazov-Elkan, A.; Balogh, D.; Willner, I. Analysis of Telomerase by The Telomeric Hemin/G-Quadruplex-Controlled Aggregation of Au Nanoparticles in The

Presence of Cysteine. *Anal. Chem.* **2014**, *86*, 3153−3158.

(40) Niazov-Elkan, A.; Golub, E.; Sharon, E.; Balogh, D.; Willner, I. DNA Sensors and Aptasensors Based on The Hemin/G-Quadruplex-Controlled Aggregation of Au NPs in The Presence of L-Cysteine. *Small.* **2014**, *10*, 2883−2891.

(41) Golub, E.; Freeman, R.; Willner, I. Hemin/G-Quadruplex-Catalyzed Aerobic Oxidation of Thiols to Disulfides: Application of the Process for the Development of Sensors and Aptasensors and For Probing Acetylcholine Esterase Activity. *Anal. Chem.* **2013**, *85*, 12126−12133.

(42) Chang, J. F.; Li, H. Y.; Hou, T.; Li, F. Paper-Based Fluorescent Sensor for Rapid Naked-eye Detection of Acetylcholinesterase Activity and Organophosphorus Pesticides with High Sensitivity and Selectivity. *Biosens. Bioelectron.* **2016**, *86*, 971−977.

(43) Li, D.; Song, S. P.; Fan, C. H. Target-Responsive Structural Switching for Nucleic Acid-Based Sensors. *Accounts. Chem. Res.* **2010**, *43*, 631−641.

(44) Ma, F.; Liu, M.; Tang, B.; Zhang, C-Y. Sensitive Quantification of MicroRNAs by Isothermal Helicase-Dependent Amplification. *Anal. Chem.* **2017**, *89*, 6182−6187.

(45) Li, L.; Feng, J.; Liu, H. Y.; Li, Q. L.; Tong, L. L.; Tang, B. Two-Color Imaging of MicroRNA with Enzyme-Free Signal Amplification via Hybridization Chain Reactions in Living Cells. *Chem. Sci.* **2016**, *7*, 1940−1945.

(46) Jiang, Y. S.; Bhadra, S.; Li, B. L.; Ellington, A. D. Mismatches Improve the Performance of Strand-Displacement Nucleic Acid Circuits. *Angew. Chem. Int. Ed.* **2014**, *53*, 1845−1848.

Table of Contents Graphic